# Electron scattering at high momentum transfer from methane: Analysis of line shapes

Maarten Vos[a)]
*Research School of Physics and Engineering, Australian National University, Canberra, Australian Capital Territory 0200, Australia*

(Received 29 November 2009; accepted 26 January 2010; published online 18 February 2010)

The measurement of the energy distribution of keV electrons backscattered elastically from molecules reveals one or more peaks. These peaks are at nonzero energy loss and have an intrinsic width. The usual interpretation of these measurements is attractively simple and assumes billiard-ball-type collisions between the electron and a specific atom in the molecule, and the scattering atom is assumed to behave as a free particle. The peak position is then related to the mass of the scattering atom, and its width is a Compton profile of the momentum distribution of this atom in the molecule. Here we explore the limits of the validity of this picture for the case of electrons scattering from methane. The biggest discrepancy is found for electrons scattering from carbon. For electrons scattering from hydrogen the effects are substantial at relatively low incoming energies and appear to decrease with increasing momentum transfer. The discrepancy is analyzed in terms of the force the atom experiences near the equilibrium position. © *2010 American Institute of Physics*. [doi:10.1063/1.3319765]

## I. INTRODUCTION

The experiment of elastic scattering of electrons from molecules in the gas phase at high momentum transfer has recently attracted attention as the results appear to be described by a billiard ball-type collisions between the impinging electron and a single atom of a molecule.[1–9] Obviously in these experiments there is momentum transfer from the electron to the molecule, and hence the kinetic energy of the molecule will change. This change in energy is reflected in the kinetic energy of the scattered electron. However, the observed energy loss of the probing electron can be interpreted quite successfully in terms of collisions between the energetic electron and a single, free atom. That is, the energy of the scattered electron is reduced by an amount consistent with a single atom absorbing the momentum transfer (recoil), rather than the whole molecule. This interpretation is referred to as the plane-wave impulse approximation (PWIA), as the collision is sudden, and the final state of the atom is described as a plane wave (i.e., a free particle). Until now the main attention was directed on the peak areas of the different components, when either a gas mixture was used, or a single molecule consisting of atoms of different masses. The exception here is the paper by Bonham *et al.*[9] that focuses on the calculation of the line shapes based on quantum scattering theory.

In this paper we want to explore experimentally the limits of the simple picture sketched above, and study for this purpose electron scattering from methane. We measured the spectra of electrons scattered from $CH_4$ at a scattering angle of 135° and used energies of 0.75–6 keV. We observed significant deviations from the PWIA for low energy scattering from H (≈1 keV) and at 6 keV for electron scatters from the carbon atom. At energies of 2 keV and more the PWIA describes the electron-proton collision fairly well. The shape of the H and C peaks is found to be described adequately if correction terms derived theoretically in the field of neutron scattering at similar momentum transfers[10] are included.

Hence we emphasize here the strong overlap between the experiments described here and neutron scattering experiments at similar momentum transfer. The latter are described extensively in Ref. 11, and the easiest starting point for reading the neutron literature is the review paper by Watson.[12] This paper provides also a theoretical background on the validity of the PWIA. These neutron experiments are mainly restricted to condensed matter targets. We will see here that the study of gas-phase molecules has significant advantages, especially in the case of highly symmetric molecules, such as $CH_4$.

There is also a strong overlap between this electron scattering study and recent work on high-energy photoemission of $CH_4$ (Ref. 13) and $CF_4$ (Ref. 14). In the photoemission case vibrations are excited both due to the core-hole creation, which changes the equilibrium bond length ("Franck–Condon-type" excitations), and the recoil of the photoelectron. In the experiment described here the electronic structure of the target does not change, and Franck–Condon-type excitations are absent, and recoil effects can thus be studied more cleanly. Another potential advantage of the electron scattering approach, relative to photoemission experiments, is that lifetime broadening does not set an upper limit to the spectral resolution that can be obtained.

In Sec. II we sketch a rough picture of the theoretical background and explain some of the important simplifications that occur in these gas-phase experiments compared with experiments in solids and liquids. The experimental setup is described briefly and the obtained spectra are com-

a)Electronic mail: maarten.vos@anu.edu.au.

 

pared with the predictions of the PWIA model with and without the inclusion of a correction term derived from the neutron scattering field.

## II. BACKGROUND

In a scattering experiment a particle with momentum $\boldsymbol{k}_0$ and energy $E_0$ interacts with a target and the momentum $\boldsymbol{k}_1$ and $E_1$ of the scattered particle are determined. We are interested here in collisions with molecules where the momentum transfer $\boldsymbol{q}=\boldsymbol{k}_0-\boldsymbol{k}_1$ is such that $|q||r|\gg 1$ with $\boldsymbol{r}$ the internuclear separation. Interference between waves emanating from different atoms can then be neglected as, due to the small but finite size of the nuclear wave function, the phase factor $\boldsymbol{q}\cdot\boldsymbol{r}$ varies rapidly over the area occupied by the nucleus, and thus the interference term averages out to 0. The neglect of the interference terms is referred to as the incoherent approximation. In the experiments, as describe here, with electrons with an energy between 0.75 and 6 keV scattering over 135°, $\boldsymbol{q}$ varies from 26 to 74 $\text{Å}^{-1}$ (or 14–39 a.u.) and $r \approx 1$ Å, and thus the incoherent approximation is valid.

In the experiment it is observable which electron scattered from C or H due to the difference in the energy after the collision. The "simplistic" explanation is that the recoil momentum of the (very fast "impulsive") collision is given to either the C atom or to the H atom. The scattering atom is treated as a free particle (PWIA) and hence it will acquire a kinetic energy $q^2/2M$ with $M$ the mass of the atom (assuming the atom was at rest before the collision). In this model the separation of electrons scattered over 135° from C and H varies from 1.7 ($E_0=1$ keV) to 10.4 eV ($E_0=6$ keV). Thus the C and H signals are easily separable in a modern spectrometer.

If the atom is not at rest before the collision but has momentum $\boldsymbol{p}$ then its kinetic energy changes from $p^2/2M$ to $(\boldsymbol{p}+\boldsymbol{q})^2/2M$ and the recoil energy is

$$E_r = \frac{(\boldsymbol{p}+\boldsymbol{q})^2}{2M} - \frac{p^2}{2M} = \frac{q^2}{2M} + \frac{\boldsymbol{q}\cdot\boldsymbol{p}}{M}. \tag{1}$$

Thus the mean recoil energy $\bar{E}_r$ is the recoil energy for scattering from a stationary atom, but the spectrum displays Doppler broadening. This Doppler broadening is a Compton profile of the nuclear momentum distribution. For a stationary molecule the Doppler broadening is thus related to the wave function in momentum space of the scattering nucleus bound to the molecule. It is clear that Eq. (1) implies symmetric peaks.

When the PWIA is valid one can interpret the spectrum as a Compton profile. Then it is customary to plot the spectrum not as a function of the energy loss $E$ but as a function of

$$y = (M/q)(E - q^2/2M). \tag{2}$$

This transformation is often referred to as "$y$-scaling" or "West scaling".[15] For this distribution $J(y)$ the intensity at $y$ is proportional to the probability that the target atom has a momentum component $y$ along the momentum-transfer direction $\hat{q}$.

Here we assumed that the relation between the kinetic recoil energy $E_r$ and transferred momentum is simply given by the classical relation $E_r=q^2/2M$. This is only true if the scattering particle is a free particle, and the wave function of the atom can be described by a plane wave. In our experiment the recoil energy is always less than the bond strength (≈4.3 eV for the C–H bond) and this PWIA approximation seems bound to fail, but in reality it works surprisingly well.

Within the incoherent approximation a well-defined momentum is transferred to a specific atom in the target. The question of the line shape is then equivalent to the following. Assume a well-defined momentum $\boldsymbol{q}$ is transferred to a specific (bound) atom, what is the energy distribution of the target in the final state? The energy increase in the target is mirrored in a reduction in energy of the scattered particle. In the context of neutron absorption this question was dealt with first by Lamb[16] as early as 1939, but very similar considerations apply to, e.g., neutron scattering,[10] Mössbauer spectroscopy[17] (momentum transfer due to emitted gamma), high-energy photoemission[18] (momentum transfer due to emitted electron), and electron scattering experiment as described here. In most of these discussions one deals with crystals, and the final state is described in terms of phonon excitations, and the possible final states form a continuum. In our case of a molecular target the final state is a discrete set of terms of vibrational and rotational states.

A general approach for calculating corrections to the PWIA was developed by Sears[10] in the context of neutron scattering. The first order correction on the impulse approximation predicts a peak shape $I(y)$ that is not proportional to $J(y)$ but to

$$I(y) \propto \left(1 - C\frac{d^3}{dy^3}\right) J(y). \tag{3}$$

Here the constant $C$ is equal to $M\langle\Delta V\rangle/36\hbar^3 q$ with $V$ as the total energy of the system and $\Delta$ the Laplacian with respect to the atom position. Thus for a strongly bound system the energy increases faster if an atom is moved from its equilibrium position and the correction term will be larger. One approach, used here, is to establish if final state effects are present by seeing if inclusion of the correction term provides a better description of the experimental data.

For small systems like $CH_4$ the final state can have only a restricted number of discrete energies. It is thus conceivable that the corresponding discrete energy levels could be resolved in the experimental spectrum. Indeed the calculations of Bonham *et al.*[9] for electron scattering from $H_2$ suggest that discrete structures should be visible for an energy resolution of 100 meV and cold target gas.

In order to investigate this for $CH_4$ let us consider the possible final states. The first thing to establish is how much of the recoil energy is available for excitation of the molecule. Notice that for an external observer the total momentum of the electron and molecule before and after the collision should be conserved. Thus if the molecule (mass $M_{\text{mol}}$) is stationary before the collision, it will acquire a kinetic energy $q^2/2M_{\text{mol}}$. The kinetic energy of the molecule is of the order of $kT$, and hence the assumption of a molecule initially at rest is quite good. According to the impulse ap-

proximation the peak is centered at $q^2/2M_{\text{atom}}$. Thus the energy that has to be distributed over the internal degrees of freedom of the molecule is $q^2/2M_{\text{atom}}-q^2/2M_{\text{mol}}$. For hydrogen this is only a small correction. For 135° scattering at 1 keV $\bar{E}_r=1.87$ eV and only 0.12 eV of this is dissipated by the enhancement of the kinetic energy of the molecule. In contrast, if one scatters from carbon (6 keV, 135°), $\bar{E}_r=0.94$ eV, but the largest part of this is dissipated by the enhanced kinetic energy of the molecule (0.71 eV), leaving only 0.23 eV to be distributed over internal excitations.

In general the internal excitations can be either rotational or vibrational. Rotational energy losses can be as small as ≈10 meV. Thus discrete peaks are not expected unless the energy resolution is of the order of 10 meV. An exception here is when one scatters from an atom at the center of mass of a molecule (such as C in $CH_4$). Then rotational excitations are not expected. Methane has nine vibrational modes. In three of these modes the carbon atom is stationary: $\nu_1$ (symmetric stretching mode, nondegenerate) and $\nu_2$ (symmetric bending mode, double degenerate). So transferring momentum to the carbon atom is not expected to excite these modes. Excitation of $\nu_3$ (asymmetric stretching mode $\hbar\omega=0.39$ eV, threefold degenerate) and $\nu_4$ (asymmetric bending mode $\hbar\omega=0.17$ eV, threefold degenerate) is expected. Thus a scattering experiment from C in $CH_4$ is especially attractive, as rotational excitations are absent and the number of vibrational modes that come into play is limited.

It is instructive to consider a simple model as a guide for interpreting the more complex results. The recoil energy distribution can be solved exactly for the case of a one-dimensional harmonic oscillator.[12] Let us explore how these solutions look for a harmonic oscillator with energy of 0.4 eV (roughly the energy of $\nu_3$ in $CH_4$) and typical recoil energies in our experiment. For 2 keV $e^-$ scattering from H in $CH_4$ the recoil energy is 3.7 eV, but 0.23 eV will be taken up by the molecule as translational kinetic energy. For internal excitations on average 3.5 eV is available. For 6 keV $e^-$ scattering from C in $CH_4$ the recoil energy is 0.94 eV, but 0.71 eV is taken up as translational kinetic energy of the molecule, hence only 0.24 eV is available for internal excitations.

Thus we want to compare our spectrum with that of scattering from a one-dimensional oscillator at a momentum transfer that corresponds with the energies available for internal excitations. The exact solution is just a Poisson distribution:[12] the probability that the harmonic oscillator with energy $\omega_o$ is in the $n$'s excited state is given by

$$e^{-\lambda}\frac{\lambda^n}{n!}, \tag{4}$$

with $\lambda=\omega_o/\bar{E}_r$ and the spectra consist of the corresponding set of delta functions at energies (in the laboratory frame), as plotted in Fig. 1. Also plotted in this figure is the shape of the spectrum when this distribution is measured with an energy resolution of 0.5 eV. The discrete structures are not observed, but the resulting line shape is clearly asymmetric especially when the recoil energy is of the order of the characteristic energy $\hbar\omega$ of the oscillator.

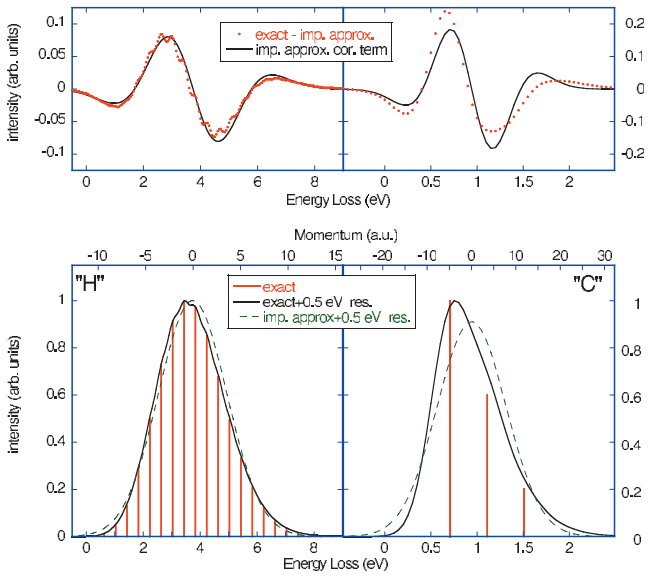


FIG. 1. The results of a model calculation for a one-dimensional harmonic oscillator for a recoil energy of 3.5 eV (typical for an electron scattering from H at 2 keV) and 0.23 eV (typical for an electron scattering from C at 6 keV). The exact solution (a set of delta functions with different amplitudes separated by $\hbar\omega$) resembles in an experiment a continuous distribution if the energy resolution is less than $\hbar\omega$ of the oscillator. The broadened exact solution differs in shape somewhat from the Doppler profile based on the momentum density of the oscillator in momentum space, as is obtained in the impulse approximation. This difference is more pronounced for recoil energies typical for scattering from C compared with those from H. The difference between exact solution (broadened by energy resolution) and the impulse approximation resembles the third derivative of the Gaussian Doppler profile, as is shown at the top panels. The lower panels also show the momentum of the scattering atom, as obtained by the $y$-scaling procedure [Eq. (2)].

If one assumes that the final states are plane waves, then the spectrum would resemble the Compton profile of the momentum density of the scattering atom. For a harmonic oscillator in the ground state the momentum density (i.e., the modulus square of the wave function in momentum space) is just a Gaussian

$$I=Ce^{-y^2/M\omega_0}, \tag{5}$$

which, with $y=(M/q)(E-\bar{E}_r)$, results in a spectrum proportional to $e^{-(E-\bar{E}_r)^2/2\omega_0\bar{E}_r}$. Thus we plotted in Fig. 1 also these corresponding Compton profiles. There are small differences between the broadened exact solution and the PWIA for the case of 2 keV electrons scattering from H in $CH_4$. The difference of both calculations (normalized to equal area) has a shape that resembles the third derivative of the Gaussian corresponding to momentum distribution, as expected based on the leading correction term derived by Sears.

For the parameters corresponding to 6 keV $e^-$ scattering of C, the differences between the broadened, exact solution and the PWIA are larger. Again the difference is fairly well reproduced by the third derivative of the Gaussian corresponding to the PWIA solution. We will show that the actual experimental results resemble these one-dimensional model calculations quite well.

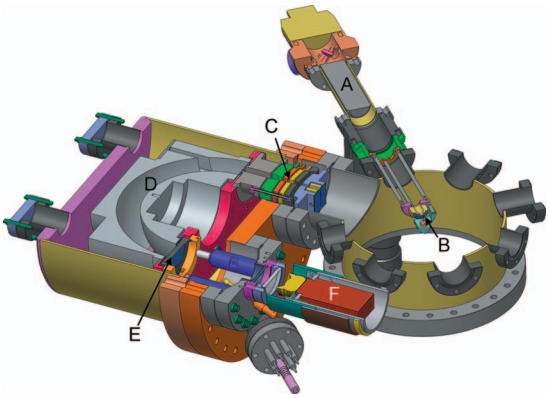


FIG. 2. A schematic view of the spectrometer showing the (a) electron gun, (b) beam defining aperture and gas jet, (c) retarding slit lenses, (d) hemispherical analyzer, (e) phosphor screen, and (f) camera.

## III. EXPERIMENTAL DETAILS

The spectrometer (shown in Fig. 2) was described in detail in Ref. 19. Since then the readout of the two-dimensional detector was changed from a resistive anode to a phosphor screen/camera.[20] Further the width of the entrance slit of the hemispherical analyzer (positioned after the slit lens) was reduced from 3 to 0.5 mm. These changes resulted in an improved full width at half maximum (FWHM) of the elastic peak of heavy targets, such as Xe where Doppler broadening is small, to 0.3 eV at modest beam current (100 nA) and 0.4 eV at larger beam currents (600 nA).

The scattering angle $\theta$ was 135°. As $|\boldsymbol{k}_0| \approx |\boldsymbol{k}_1|$ the magnitude of the momentum transfer is $|q| = 2|k_0|\sin(\theta/2) = 2|k_1|\sin(\theta/2)$ (see, e.g., Ref. 21). Note that in photoemission the magnitude of the recoil is $|\boldsymbol{k}_1|$ (the momentum of the photoelectron). Thus a 1000 eV scattering experiment as described here has the same recoil momentum as a 3400 eV photoelectron. The recoils probed here are thus substantially larger than those of the reported photoemission experiment on $CH_4$ (Ref. 13) and $CF_4$ (Ref. 14).

An important consequence of the camera readout is a much more uniform response of the detector. This makes it possible to take reliable data with the offset voltage scanning over only a few volts. The region of interest (from −1 eV to, say, 5 eV energy loss) is then always within the 20 eV detection window of the analyzer, operating at 200 eV pass energy. The intensity measured when the gas enters the chamber, not through the needle pointing toward the interaction region but through a side port, is much reduced and flat. Hence we fit the data by a peak structure and a very small constant background. This speeds up the measurement fourfold compared with the original mode of operation where the complete region of interest was scanned over the whole of the detector, and a background measurement was done for equal duration as the signal measurement. In spite of this some of the high-energy runs took more than a week. At low incoming energies, where the cross sections are larger, measurements were done both by scanning over the whole detector plus separate background run, or by scanning over only a small part of the detector, and very similar results were obtained.

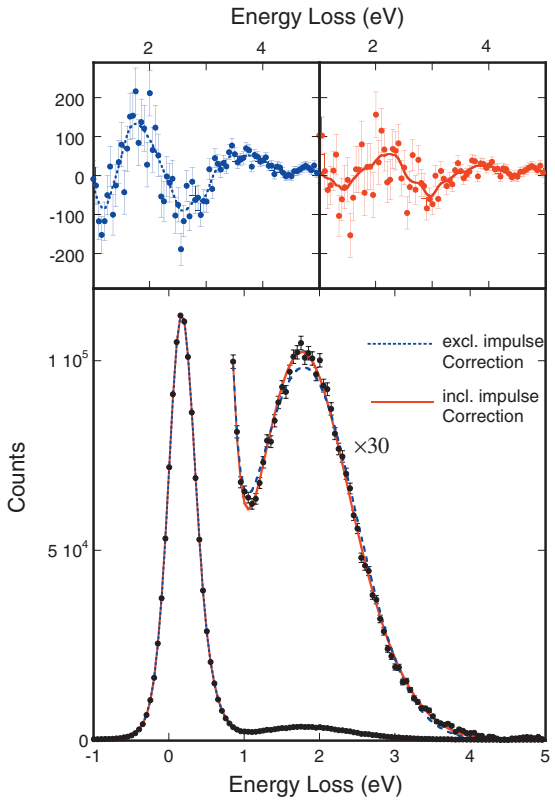


FIG. 3. Spectrum for 1 keV $e^-$ scattering from $CH_4$. The focus is on the H peak which is fitted with (full line) and without an impulse correction term. The residuals are shown at the top panel for the energy range corresponding to the H peak (left without impulse correction, right with impulse correction). The line in the residual plot is obtained by smoothing and is a guide to the eye only.

Either pure methane or a 2:1 mixture of helium and methane was used for the measurement. In one occasion a small amount of ≈1% of Xe was added to this mixture. The exact zero of the energy loss scale depends on details of the lens settings and cathode work function. For He we scatter from a truly free particle, and hence we know its recoil energy $q^2/2M_{\mathrm{He}}$. From the He peak position we can fix the zero energy loss position of the energy scale. This works only for larger incoming energies (above 2 keV) as below 2 keV the He signal is not separated from the C signal. The same applies for Xe, but the Xe signal is only separated from the C signal at the highest energies (6 keV).

## IV. RESULTS

### A. Hydrogen peak shape

In Fig. 3 we show the spectra of 1 keV $e^-$ scattering from methane. Two peaks are seen, a large one followed by a broader and much weaker one at ≃1.7 eV larger energy loss. The first peak is attributed to carbon, the second one to hydrogen. The carbon peak is stronger, as the elastic scattering cross section roughly scales as $Z^2$. The zero point of the energy scale is adjusted so that the C peak is at an energy loss of $q^2/2M_{\mathrm{C}}$. At 1 keV the width of the carbon peak is very close to the width of the Xe peak, measured separately to establish the resolution of the spectrometer. Our analysis focuses thus on the hydrogen peak, which is much broader

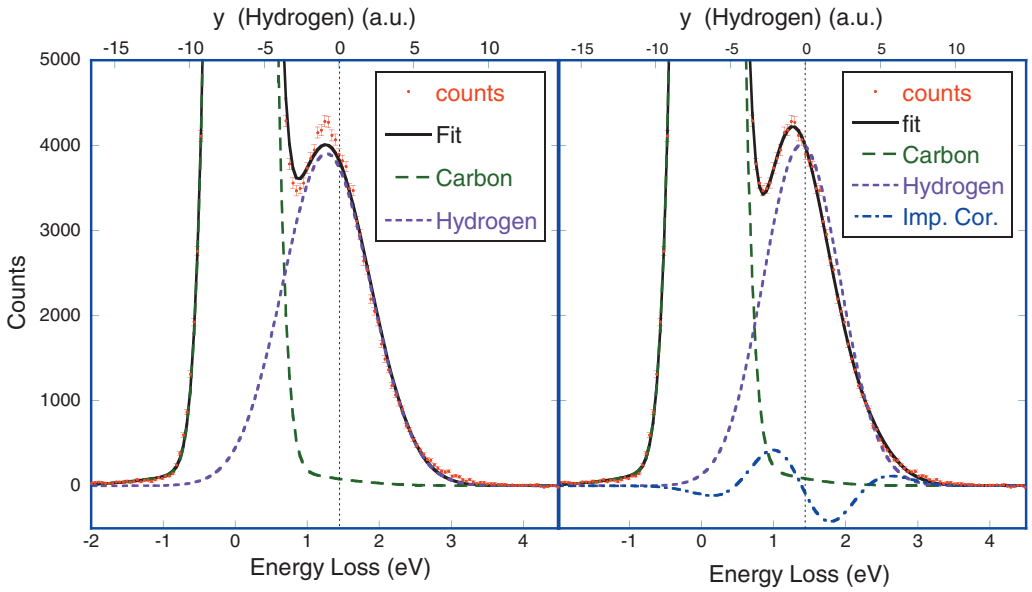


FIG. 4. The fitting procedure illustrated for $E_0=750$ eV measurement, as described in the main text.

than the spectrometer resolution, to see if the H line shape is a Compton profile of the H momentum distribution. A necessary requirement for this is a symmetric peak shape, as the H momentum is equally likely to be directed in any direction (hence, positive values of $\boldsymbol{q}\cdot\boldsymbol{p}$ [see Eq. (1)] are as likely as the corresponding negative ones). A Gaussian peak shape is expected as the potential will be close to harmonic near the H equilibrium position. The spectra were thus fitted with a Gaussian. The residuals are shown at the top panel of Fig. 3. The fit is reasonable, but the residuals show a clear structure. We then checked if the quality of the fit improves if we include first-order correction term [see Eq. (3)]. Indeed the fit improves, and the most obvious structure in the residuals disappears.

These effects are stronger at lower energy. We illustrate the fitting procedure in Fig. 4 for the lowest energy (750 eV) measurement. The H peak approached the main C peak, but is still resolved. We use the C peak to fix the zero of the energy scale by assuming it is at $q^2/2M_C$. Then we can calculate the momentum scale of the electrons scattered from H using the $y$-transform [Eq. (2)] with the $M=1$. The resulting momentum scale is shown at the top of the panels. Fitting is subsequently most easily done in momentum space. The C peak is fitted by three Gaussians centered at almost the same energy (this will be discussed later). If we fit the H part of the spectrum with a Gaussian only, then this Gaussian is not centered at zero momentum. This fit also does not mimic the measured shape well. Including the impulse correction term improves the position of the Gaussian (much closer to 0 momentum) and the shape of the spectrum is reproduced much better. Fitting in momentum space gives physically meaningful quantities for the H peak width and the impulse correction term. The C–H peak separation obtained and the C peak width itself (which width is to a large extent determined by the finite energy resolution of the spectrometer) are meaningful in energy space. For these quantities the momentum space values are transferred to energy space by multiplying by $q/M_H$.

The same procedure was followed for other incoming energies and the results for a 2 keV measurement are shown in Fig. 5. Now the fit with a Gaussian is quite good, and the improvement of the fit by the addition of final state corrections is marginal.

A comparison of the measurement and the one-dimensional model calculation (Fig. 1) shows a qualitative agreement. The magnitude of the correction term should scale as $1/q$ or $1/\sqrt{E_0}$. The impulse correction is plotted

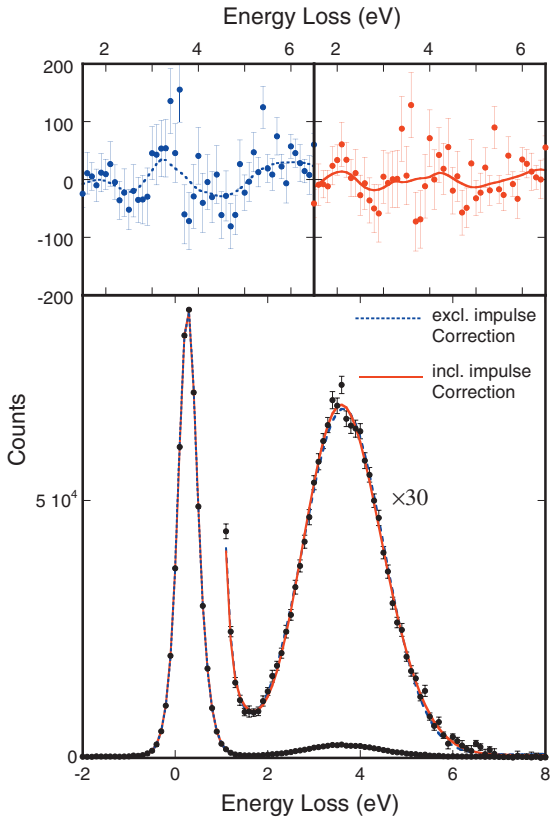


FIG. 5. Same as in Fig. 3, but for $E_0=2$ keV.

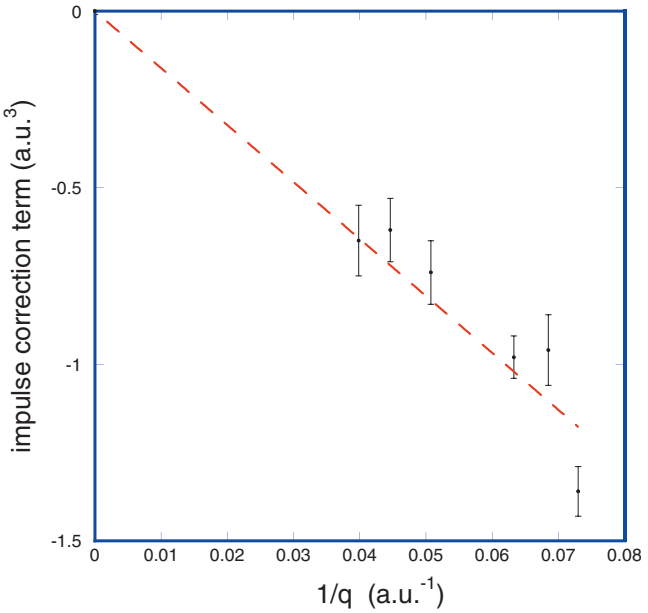


FIG. 6. The magnitude of the impulse correction plotted vs $1/q$. The theory of Sears (Ref. 10) predicts a linear dependence of the impulse correction on $1/q$.

versus $1/q$ together with a linear fit through the origin (Fig. 6). The correction term appears to be proportional to $1/q$ but different approaches of fitting the carbon part of the spectrum may result in slightly different values for the impulse correction term.

The results obtained from the fits are summarized in Table I. Unless otherwise stated these results were derived from fits including the final state correction. The intensity ratio of the C and H elastic peak ($I_C/I_H$) was discussed extensively in a previous publication.[5] For completeness we also reproduce this ratio as well in the table and compare it with expectations based on calculated atomic elastic scattering cross sections as obtained using the ELSEPA program of Salvat *et al.*[22] Absorption effects were included in the calculation. Agreement with the experiment is within ≈5%, indicating that these cross section ratios can be derived from atomic cross sections. These measurements extend to lower energy, compared with those in Ref. 5. The calculated increase in $I_C/I_H$ with decreasing $E_0$, predicted by ELSEPA, seems to be confirmed by the experiment. For the highest $E_0$ values the experimental and calculated ratio approaches 9, the value one obtains if one approximates the elastic scattering cross section by the Rutherford cross section.

From the table it is clear that the width of the H peak in momentum space is fairly constant, in agreement with the interpretation of $J(y)$ as a Compton profile. In energy space the width of the H peak increases proportional to $q$. The separation of the C and H peaks obtained from the fits is given as well, both for with (labeled imp. cor.) and without (labeled PWIA) impulse corrections. Note that the agreement of the shift with the predictions of Eq. (1) is better if final state corrections are included.

The fact that the correction terms are small, especially at larger values of $E_0$, indicates that interpretation of these measurements in terms of a Compton profile of the proton momentum distribution is reasonable. There is then a simple relation between the peak width ($\sigma$) and the mean kinetic energy of the proton. It is given by

$$\sigma_{\mathrm{Dop}} = \sqrt{(4/3)\langle E_{\mathrm{kin}}\rangle \overline{E_r}}. \tag{6}$$

The derived values for $E_{\mathrm{kin}}$ obtained from Eq. (6) are shown in Table I as well. Moreh and Nemirovsky[7] discussed extensively the mean kinetic energy of H in $CH_4$. They obtained a value of 148 meV at room temperature and 135 meV at 0° K. The mean value of the experiment (≈151 meV) is consistent with the room temperature value in Ref. 7 (the difference in value obtained at different energies can be seen as an indication of the accuracy of the measurement and fitting procedure). However the calculated value is based on the assumption that the molecules have an energy of $0.5kT$ for each translational degree of freedom, whereas the momentum distribution of the atoms leaving the needle is far from statistical equilibrium, and we will come back to this later.

### B. Carbon peak shape

For C the shifts and broadening are much smaller than for H. For our analysis of the H component we used the C peak to establish the zero point of the energy scale (i.e., assumed that the C peak was at $q^2/2M_C$). For investigating the C peak shape it is necessary to establish the zero point more accurately. For this purpose we used a 1:2 mixture of

TABLE I. The results for the hydrogen peak in $CH_4$ for various incoming energies $E_0$ and the corresponding momentum transfer $|q|$. First the measured and calculated peak area ratio $I_C/I_H$ of the carbon and hydrogen-derived elastic peaks. The peak width (corrected for experimental resolution between parentheses), observed and calculated C–H peak separation ($\Delta E$), mean kinetic energy of the H atoms obtained using Eq. (6) ($\overline{E_r}$), as well as the magnitude of the derived final state corrections. The 6 keV measurement was taken from Ref. 5, but at these high energies the cross sections are too low to derive a meaningful value of the impulse correction term.

| $E_0$ (keV) | $\lvert q\rvert$ (a.u.) | $I_C/I_H$ Obs. | $I_C/I_H$ Calc. | $\sigma_H$ (a.u.) | $\sigma_H$ (eV) | $\Delta E_{\mathrm{expt}}$ (eV) (Imp. cor.) | $\Delta E_{\mathrm{expt}}$ (eV) (PWIA) | $\Delta E_{\mathrm{calc}}$ (eV) | $\overline{E_{\mathrm{kin}}}$ (meV) | Imp. cor. (a.u.$^3$) |
|---|---|---|---|---|---|---|---|---|---|---|
| 0.75 | 13.7 | 11.3 | 10.7 | 2.61 | 0.53(0.51) | 1.26 | 1.14 | 1.29 | 151 | 1.36 ± 0.07 |
| 0.85 | 14.6 | 10.5 | 10.6 | 2.73 | 0.59(0.57) | 1.38 | 1.31 | 1.46 | 168 | 0.96 ± 0.10 |
| 1.00 | 15.8 | 10.5 | 10.5 | 2.69 | 0.63(0.61) | 1.68 | 1.61 | 1.71 | 144 | 0.98 ± .06 |
| 1.55 | 19.7 | 10.3 | 9.95 | 2.63 | 0.76(0.73) | 2.60 | 2.57 | 2.66 | 150 | 0.74 ± .06 |
| 2.00 | 22.4 | 10.2 | 9.6 | 2.58 | 0.86(0.83) | 3.39 | 3.35 | 3.44 | 151 | 0.62 ± .09 |
| 2.50 | 25.1 | 10.0 | 9.4 | 2.57 | 0.98(0.95) | 4.32 | 4.28 | 4.30 | 144 | 0.65 ± 0.1 |
| 6.00 | 38.9 | 9.2 | 9.1 | 2.62 | 1.55(1.50) | ⋯ | 10.48 | 10.36 | 149 | ⋯ |

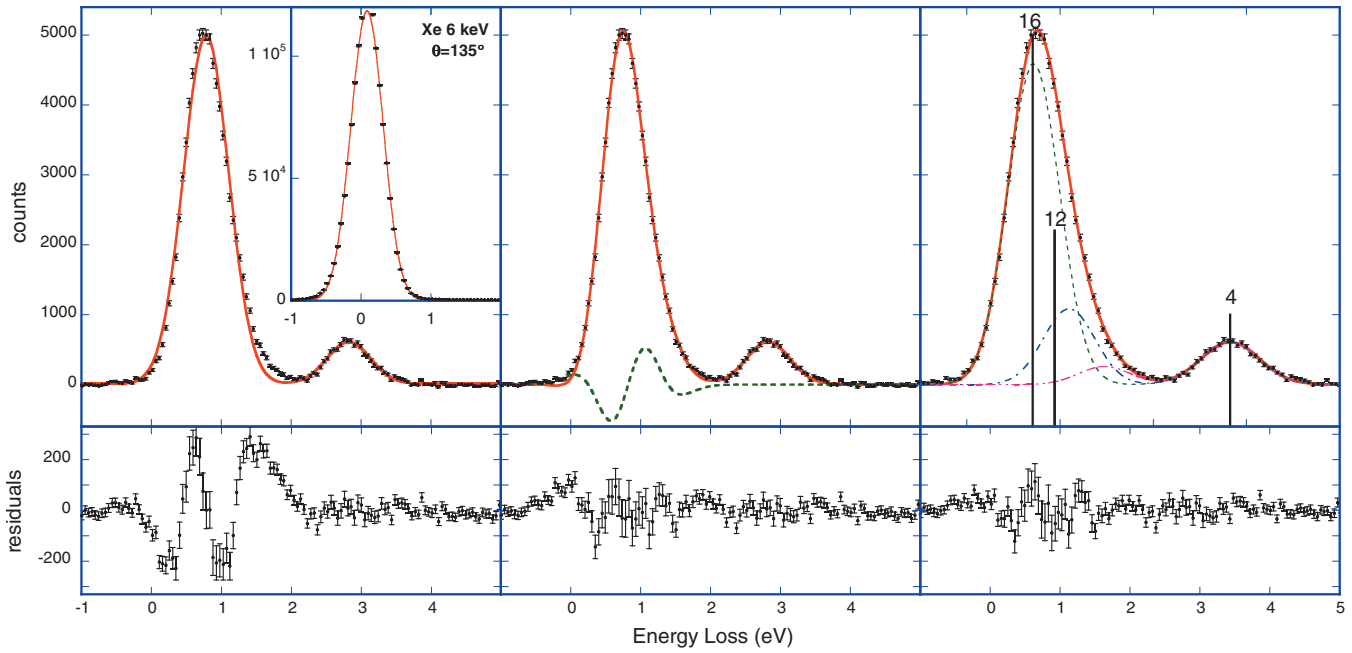


FIG. 7. Various analysis of the carbon peak in a 6 keV, 135° scattering experiment. A $CH_4$ He mixture was used and the He peak near 2.8 eV is used to fix the zero of the energy scale. In the left panel the C peak is fitted with a single Gaussian, in the central panel with a single Gaussian and its third derivative. In the right panel we fit the C peak with two Gaussians with energy positions fixed as explained in the main text. The residuals of each fit are shown in the lower panels. A Xe spectrum, fitted with a single Gaussian, taken under identical conditions is shown as an inset.

$CH_4$ and He. The results of the 6 keV measurement shown in Fig. 7 show two peaks separated by ≈2.0 eV. The hydrogen peak is now at ≃11 eV energy loss[5] and is thus not contained in this measurement. We associate the two peaks with scattering from C and He. In the PWIA the expected separation of these peaks is 1.88 eV. The C elastic cross section is $\approx Z_C^2/Z_{He}^2=9$ times the cross section of He, hence the C peak is larger, in spite of the fact that twice as much He is present. The He and C peaks have a comparable width ($\sigma\approx 0.33$ eV), but it is considerably more than the width measured for Xe under the same experimental conditions ($\sigma\approx 0.22$ eV). Results are summarized in Table II.

Based on the translational motion alone we expect, assuming a momentum distribution in thermal equilibrium and Eq. (6), a broadening ($\sigma$) of 0.19 eV for $CH_4$ and 0.37 eV for He. Clearly the observed He peak (including experimental broadening) is considerably narrower than the predicted value based on equilibrium thermal motion. For Xe, measured in a separate experiment, the predicted thermal broadening would be only 0.065 eV (due to its large mass), and hence we take the observed Xe width ($\sigma=0.23$ eV, i.e., 0.54 eV FWHM) as the estimate of the spectrometer resolution. Subtracting the energy resolution (in quadrature) leaves for the case of He 0.23 eV due to thermal translational motion. Thus cooling and/or collimation of the motion of the gas emerging from the gas jet has a significant effect on the observed width. The C width ($\sigma$) corrected for energy resolution is then 0.24 eV. This is slightly more than the expected width (0.19 eV) due to translational motion, even when one assumes a room temperature distribution. Thus the excess width is resolved which is of the order of the vibrational energies.

TABLE II. The results for Xe, C, and He for run (a) (Xe measured in a separate run from the $CH_4$–He mixture) and run (b) (using a Xe–$CH_4$–He mixture). For C the value in parenthesis is the measured width corrected for energy resolution based on the Xe width. The mean kinetic energy of C is obtained from this corrected value using Eq. (6) and is closer to the calculated mean kinetic energy at 0 K (47.3 meV) than the calculated room temperature value (76.3 meV) (Ref. 7).

| Run | $\sigma$ Xe (eV) | $\sigma$ C (eV) | $\sigma$ He (eV) | $\overline{E_{kin}}$ C (meV) |
|---|---|---|---|---|
| a | 0.23 | 0.33 ± 0.03 (0.24) | 0.33 | 46 ± 12 |
| b | 0.21 | 0.33 ± 0.03 (0.25) | 0.32 | 52 ± 12 |

The widths mentioned here were extracted from a fit of the He and C peaks, each with a single Gaussian. This is shown in Fig. 7. The He peak is well described by a single Gaussian, but the carbon peak deviates in a systematic way. The actual peak is sharper than the Gaussian at the low energy loss side and less steep at the large energy loss side. The residuals shown at the top panel of Fig. 7 are again very reminiscent of the difference between the exact and PWIA solution of the one-dimensional oscillator. Hence it was investigated if inclusion of a final state effect correction term proportional to the third derivative of the Gaussian would improve the fit. This is indeed the case, as can be seen in the central panel. A third approach is to consider the possible final states. As rotational excitations are not expected, when scattering from the center of mass of a molecule, and the translational energy changes by $q^2/2M_{mol}$, we can calculate the energy loss for when the molecule is left in its vibrational ground state, first excited state, etc. Using the peak position of He to fix the zero of the energy loss scale we can try to fit the spectrum with only the probability of leaving the molecule in a certain vibrational state as a fitting parameter. This is done in the right panel of Fig. 7 where only vibrational

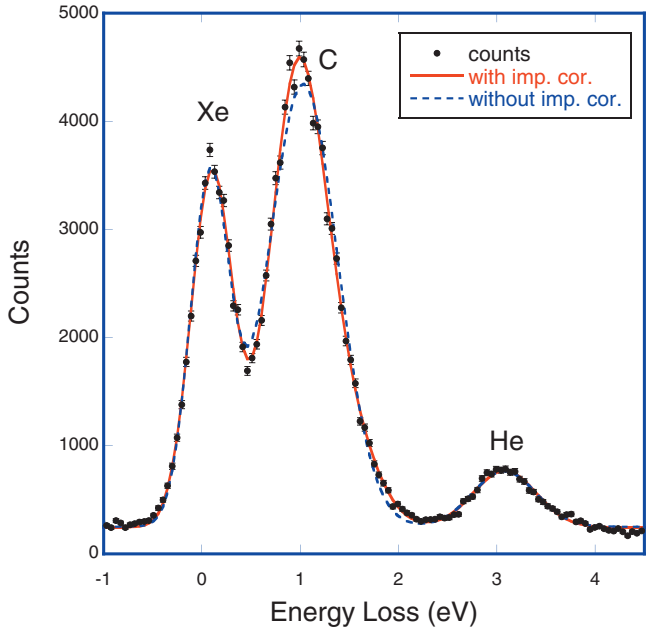


FIG. 8. Spectra of a 2:1 mixture of $CH_4$ and He with an additional 1% of Xe added ($E_0$=6 keV).

mode $\nu_3$ was considered. A good fit with reasonable amplitudes is obtained, reminiscent of the exact solution of the harmonic oscillator. As stated before, it is expected that $\nu_4$ is also excited. Good fits with both vibrational modes are possible as well, but the fits are far from unique. It is necessary to improve the energy resolution by at least a factor of 2 if one really wants to determine the probability that the molecule is left in a specific vibrational final state.

If we assume, in spite of the reservations on the validity of the PWIA, that we can extract the mean kinetic energy of the C atom using Eq. (6), then we obtain a mean kinetic energy of 46–52 meV. This is substantial less than calculated in Ref. 7 for C in $CH_4$ at room temperature (76.3 meV) and close to the calculated values for 0 K (47.3 meV).

Finally we added ≈1% of Xe to the gas mixture and obtained spectra, as shown in Fig. 8. Due to the large cross section of Xe, such a low concentration of Xe still gives a large contribution to the spectrum. Now three peaks are observed (Xe, C, and He peaks, the H peak is at much larger energy loss). Again the C peak is clearly broader than the Xe peak. Also a fit of the three peaks by three Gaussians gives satisfactorily results for the He and Xe peaks, but the C peak again shows the familiar deviations from a Gaussian peak shape. Adding an impulse-correction term to the C peak results in a good fit of the whole spectrum. Thus again the fact that the C atom is part of a molecule seems to cause an asymmetry to the line shape. The separation of the He and Xe peaks was somewhat larger (0.2 eV) than the calculated values of $\bar{E}_r$. This seems to indicate that the velocity distribution of the gas leaving the needle has some influence on their peak position. The cause of this deviation is under further investigation.

The obtained widths of this experiment are reproduced in Table II as well. These values are slightly different from the measurement shown in Fig. 7, indicating small variations in experimental resolution between different runs. Again an intrinsic carbon width of 0.25 eV was obtained.

## V. DISCUSSION AND CONCLUSION

We have presented experimental results for electrons scattering from methane at high momentum transfer. The hydrogen peak is fairly well described by a Gaussian, only at the lowest scattering energies there are clear indications that the H peak shape is affected by the fact that H is bound to a molecule.

The width of the He peak is less than that expected for He gas in equilibrium at room temperature. This is attributed to a collimation effect of the beam exiting the needle, hence reducing the translational momentum component along $\boldsymbol{q}$. In this light it is at first sight somewhat surprising that we do not see the same reduction in the width of the proton peak in $CH_4$. The observed value is in line with expectations for scattering from methane with an equilibrium room temperature momentum distribution. The predicted difference in width between room temperature and 0 K is only ≃8%,[7] and this is slightly larger than the scatter in the mean kinetic energy obtained for different values of $E_0$. The kinetic energy of a H atom due to rotations is at room temperature, about four times larger than the kinetic energy due to translation.[7] It is to be expected that collimation effects do not affect the rotational energy of the molecule. Hence the effect of collimation for H should be much less than the calculated difference in mean kinetic energy at room temperature and 0 K, in agreement with our measurement.

For electrons scattering from C we can only resolve clearly the intrinsic width of the C signal at the highest scattering energies used. However, under these conditions we find fairly substantial deviations of the C peak shape from Gaussian. These results can be made plausible by model calculations using a one-dimensional harmonic oscillator. Asymmetries are important if the energy available for internal excitations is of the order of the characteristic energy of these excitations. If the energy scale of all internal excitations is much smaller than the energy available for internal excitations, we obtain a symmetric profile, and then the profile can be interpreted as a Compton profile of the nuclear momentum density.

If we extract the mean kinetic energy of the C atom from the 6 keV experiment, in spite of our reservation of the validity of the PWIA, then the obtained value is closer to the 0 K prediction than the room temperature prediction.[7] Thus in this case collimation effects seem important. This can be explained by the fact that, in contrast to H, the rotational excitations do not affect the mean kinetic energy of a carbon atom, and hence collimation effects are not obscured by larger kinetic energy contributions of the rotational modes. Thus the agreement between the experimentally obtained value and the theoretical prediction is as good as can be expected under these conditions. For a more precise comparison it would be required to use higher momentum transfer [which means the PWIA is more applicable and the width

(in eV) of the Compton profile increases] and preferably the use of a gas cell, where the momentum distribution is closer to thermal equilibrium.

For scattering of electrons from protons in $CH_4$ we expect rotational excitations to be important, and hence it is questionable if discrete features can be resolved if the overall energy resolution is larger than the spacing of the vibrational levels. For scattering from C the prospect of resolving discrete structures with improved energy resolution is brighter, as rotational excitations are not expected if the recoil is transferred to the center of mass of the molecule.[14] Thus if the resolution is improved to 100 meV, or less, then discrete pictures should be visible in the spectrum. It will then be even more interesting to compare the measured spectra with truly microscopic theories [such as described by Bonham *et al.* for the case of $H_2$ (Ref. 9)] to test our understanding of these processes based on quantum physics, rather than the semiclassical PWIA, which works surprisingly well at high energies and modest energy resolution.

## ACKNOWLEDGMENTS

The author wants to thank R. Bonham, C. A. Chatzidimitiou-Dreismann, G. Cooper, A. Hitchcock, R. Moreh, D. Thomas, and E. Weigold for stimulating discussions and/or critical reading of the manuscript. The research was made possible by funding from the Australian Research Council.

[1] M. Vos, G. Cooper, and C. Chatzidimitriou-Dreismann, in *Electron and Photon Impact Ionization and Related Topics*, Institute of Physics Conference Series Vol. 183, edited by B. Piraux (Institute of Physics Publishing, Bristol, 2005), pp. 81–91.
[2] G. Cooper, A. Hitchcock, C. Chatzidimitriou-Dreismann, and M. Vos, J. Electron Spectrosc. Relat. Phenom. **155**, 28 (2007).
[3] G. Cooper, E. Christensen, and A. P. Hitchcock, J. Chem. Phys. **127**, 084315 (2007).
[4] G. Cooper, A. P. Hitchcock, and C. A. Chatzidimitriou-Dreismann, Phys. Rev. Lett. **100**, 043204 (2008).
[5] M. Vos, M. Went, G. Cooper, and C. Chatzidimitriou-Dreismann, J. Phys. B **41**, 135204 (2008).
[6] M. Vos and M. Went, J. Phys. B **42**, 065204 (2009).
[7] R. Moreh and D. Nemirovsky, J. Chem. Phys. **130**, 174303 (2009).
[8] R. Moreh and D. Nemirovsky, J. Chem. Phys. **131**, 054305 (2009).
[9] R. Bonham, G. Cooper, and A. P. Hitchcock, J. Chem. Phys. **130**, 144303 (2009).
[10] V. F. Sears, Phys. Rev. B **30**, 44 (1984).
[11] C. Andreani, D. Colognesi, J. Mayers, G. F. Reiter, and R. Senesi, Adv. Phys. **54**, 377 (2005).
[12] G. I. Watson, J. Phys.: Condens. Matter **8**, 5955 (1996).
[13] E. Kukk, K. Ueda, U. Hergenhahn, X.-J. Liu, G. Prümper, H. Yoshida, Y. Tamenori, C. Makochekanwa, T. Tanaka, M. Kitajima, and H. Tanaka, Phys. Rev. Lett. **95**, 133001 (2005).
[14] T. D. Thomas, E. Kukk, R. Sankari, H. Fukuzawa, G. Prümper, K. Ueda, R. Püttner, J. Harries, Y. Tamenori, T. Tanaka, M. Hoshino, and H. Tanaka, J. Chem. Phys. **128**, 144311 (2008).
[15] G. B. West, Phys. Rep. **18**, 263 (1975).
[16] W. E. Lamb, Phys. Rev. **55**, 190 (1939).
[17] B. Kaufman and H. Lipkin, Ann. Phys. (N.Y.) **18**, 294 (1962).
[18] Y. Takata, Y. Kayanuma, M. Yabashi, K. Tamasaku, Y. Nishino, D. Miwa, Y. Harada, K. Horiba, S. Shin, S. Tanaka, E. Ikenaga, K. Kobayashi, Y. Senba, H. Ohashi, and T. Ishikawa, Phys. Rev. B **75**, 233404 (2007).
[19] M. Vos, M. R. Went, Y. Kayanuma, S. Tanaka, Y. Takata, and J. Mayers, Phys. Rev. B **78**, 024301 (2008).
[20] M. Vos, M. Went, and E. Weigold, Rev. Sci. Instrum. **80**, 063302 (2009).
[21] M. Vos, Phys. Rev. A **65**, 012703 (2001).
[22] F. Salvat, A. Jablonski, and C. J. Powell, Comput. Phys. Commun. **165**, 157 (2005).